

High-resolution spectra of atmospheric water vapor in the near-IR using a Raman-shifted alexandrite laser

Marc R. Hammond, Thomas D. Wilkerson, and Vincent B. Wickwar
Center for Atmospheric and Space Sciences, Utah State University, Logan, UT 84321

ABSTRACT

We have developed a pulsed, narrow line Raman shifted alexandrite laser to produce tunable near-IR radiation in the 1140 nm absorption band of water vapor. With the first Stokes Raman conversion in hydrogen, the full tuning range of alexandrite, 730-790 nm, can potentially cover the wavelength range 1050 –1200 nm. The application to differential absorption lidar, DIAL, is the vertical profiling of humidity and temperature in the atmosphere. This paper reports the application of Raman-shifted alexandrite radiation for new quantitative measurements of the strengths and widths of water vapor absorption lines between 8865 and 8915 cm^{-1} . These results will be presented. Alexandrite wavelength determination was obtained with oxygen A-band rotational lines near 765 nm. Similar applications and studies of the water vapor band near 940 nm can be readily carried out by Raman-shifting in deuterium.

Keywords: Water vapor, linestrengths, air-broadened halfwidths, Alexandrite, Raman, DIAL

1. INTRODUCTION

A number of new or improved approaches to lidar remote sensing of the troposphere are now possible owing to advances in laser technology and new techniques in the last decade. Of particular importance to atmospheric measurements is the *Differential Absorption Lidar* technique where multichannel laser remote sensing allows direct temperature and density profiling given *a priori* knowledge of molecular line parameters. In this work, we have concentrated our efforts on the development of a broadly tunable (100 nm) near-infrared laser transmitter having a sufficiently narrow line width to measure the absorption lines of H_2O , O_2 , and metallic species of the troposphere, stratosphere, and mesosphere. We used this new platform to measure H_2O line parameters and compared the results to the current *High-resolution Transmission* database (HITRAN). The database, regarded as the industry standard in molecular line parameter compilation, is important to the successful operation of any DIAL system.

In 1973 the HITRAN database was first made available to the public and has since then become the standard model for spectroscopic properties of the atmosphere¹. While the spectroscopic parameters for O_2 have been trusted by the community for many years now, recent studies^{2,3,4} have suggested that the quoted values for the near-infrared water lines need to be reconsidered. Historically, water vapor spectral measurements in the near-IR region just beyond 1000 nm are sparse owing to the lack of good light sources and detectors at those wavelengths. There are currently no broadly tunable sources which directly operate in the near-IR so there has been an impetus to develop technology to access this part of the spectrum⁵. Early HITRAN compilations of H_2O lines were constructed mostly from solar spectrum, and laboratory efforts by Giver et al. in 1982 of the 940 nm band showed good agreement for 97 lines observed⁷. In 1993, the 940 nm band was measured with a Raman shifted dye laser for comparison with HITRAN-91 version⁸. In that work, 45 line strengths (6% average uncertainty) and 30 line widths (8% average uncertainty) were measured. The HITRAN-91 line strengths consisted of values measured from solar spectrum analyses⁹ and were found to be in agreement with experiment to 3%. The 30 measured widths were found to be a factor of 1.059 larger on average than the HITRAN-91 values. Historically, experimental comparisons to the HITRAN database have shown favorable agreement for the 940 nm band.

Recent theoretical work in the 1140 nm band has been more controversial. In 1995, intensity calculations made by Lynas-Gray et al. were compared to HITRAN database entries from which it was suggested that the HITRAN intensity errors were thought to be less than 10% in most cases but may be as high 50% in a few cases¹⁰. The most recent theoretical calculations of line positions and intensities¹¹ provide the most accurate and extensive treatment of the water problem to date. Line positions and intensities for over 30,000 lines were calculated and compared to the HITRAN 96 database. While the total sum of intensities for the calculations were in good agreement with HITRAN, the individual band sums have significant variations. The summed intensities for the lines in the (111-000) vibrational band were reported to be a factor of 1.33 larger than corresponding HITRAN entries. These lines are of interest since our measurements included lines mostly from this band. The overall trend in empirically and theoretically determined line strengths suggests that HITRAN line strengths for H_2O may be under-predicted in the 1140 nm band. Contrary to this trend is the recent work by Giver et al.⁴ whose conclusions suggested HITRAN H_2O line strengths were slightly over-predicted.

More recent literature on near-IR water vapor line strengths and widths include theoretical predictions, which in some cases are in poor agreement with direct measurements. The present near-IR compilations of line strength data in HITRAN-2000 are those of Giver et al.⁴ This update was motivated by systematic differences found between HITRAN-96 and the corresponding literature used to make up the database. The widths listed for the (111-000) vibrational band are mostly compiled from theoretical work done by Gamache and Davies¹². The tabulation of widths in HITRAN are in the form N2-broadened half widths, self-broadened half widths, and a temperature exponent for N2-broadening¹³. From these line-by-line data, the total width of a line is calculated for a given temperature and pressure. In our work, we did not explore the accuracy of the temperature exponent due to time constraints. Most work on HITRAN validation has been done at a “reference temperature” which occurs in the HITRAN data base design as a fiduciary temperature (296 K).

We have developed a tunable laser DIAL transmitter using a pulsed alexandrite laser. The suitability of this laser as the preferred light source for near-IR DIAL observations has recently been demonstrated by Wulfmayer et al.¹⁴[1995]. The first important application of this development has been to make new measurements of 15 H₂O linestrengths and line widths for selected lines from the 2ν+δ polyad of water vapor at 1140 nm. For 15 lines in the wavenumber range 8865-8915 cm⁻¹, we find that the line strengths compared to HITRAN-2000 are a factor of 1.28 (±13%) larger on average, and the line widths comparisons are a factor of 1.13 (±21%) larger on average. The data were taken under laboratory conditions at Utah State University during October 2000. This work joins with an increasing number of efforts in the atmospheric community to review and correct the near IR data for H₂O in the HITRAN-2000 database.

2. BACKGROUND AND THEORY

Monochromatic light attenuates exponentially in the atmosphere according to the Beer-Lambert law¹⁵, which is a function of the absorption coefficient (σ), the number density (ρ) of absorbers, and the distance (x) over which the light wave travels. In the absence of aerosols, the absorption coefficient is a function of atomic and molecular transitions. The atmospheric transmittance at any point in the spectrum is determined by all contributions of atomic and molecular absorption at that frequency,

$$T(\nu) = \exp\left[-x \sum_{i=1}^N \rho_i \sigma(\nu, \nu_i)\right] \quad (1)$$

In general, an arbitrary molecular absorption line exhibits a naturally broadened Lorentzian line shape which is further broadened by thermal motion and collisions between molecules. The Voigt function, which is usually calculated through convolution of Gaussian and Lorentzian profiles, is the function used to calculate the absorption coefficient line shape. At tropospheric densities, the lineshape is predominantly collisionally broadened (Lorentzian), however for accuracy, the Voigt function is adopted here. In the 1140 nm region, H₂O is the only major absorber and the Beer-Lambert law can be solved for the absorption coefficient which is the product of the linestrength and line shape function,

$$\sum_{i=1}^N S_i f(\nu, \nu_i, \gamma_i^p, \gamma_i^T) = \frac{\ln[T(\nu)]}{\rho x} \quad (2)$$

Expressed in this way, the absorption coefficient has all the model parameters on the left-hand side of the equation and all the measured parameters on the right hand side. The absorption coefficient can then be constructed from the parameters of the HITRAN database. For computational simplicity, a closed-form approximation of the Voigt function, accurate to within 3%, was used¹⁶:

$$f = f_0 \left\{ (1-r) \exp(-2.772z^2) + \frac{r}{1+4z^2} + 0.016r(1-r) \left[\exp(-0.4z^{2.25}) - \frac{10}{10+z^{2.25}} \right] \right\} \quad (3)$$

where, r is the ratio of the pressure-broadened width and the Voigt width, γ_L/γ_V . The centerline value and parameter z are defined as:

$$f_0 = \left\{ \frac{\gamma_V}{v_0^2} \left[1.065 + 0.447r + 0.058r^2 \right] \right\}^{-1} \quad (4)$$

$$z = \frac{v_0^2}{\gamma_V} \left(\frac{1}{v} - \frac{1}{v_0} \right) \quad (5)$$

The width of the Voigt profile is expressed in terms of the pressure-broadened width, γ_L , and the Doppler width, γ_G ,

$$\gamma_V = \frac{\gamma_L}{2} + \sqrt{\left(\frac{\gamma_L}{2} \right)^2 + \gamma_G^2} \quad (6)$$

In general, line strengths and line widths are temperature dependent. In this study the temperature and pressure was not controlled so the data were modeled according to laboratory conditions from which the line strengths and widths at the reference temperature were obtained. The spectroscopic water vapor parameters were extracted from HITRAN at the reference temperature ($T_{REF} = 296$) and pressure (1 atm) and used to calculate the line strength and width for the laboratory conditions. The linestrength at any given temperature is given by

$$S(T) = S(T_{REF}) \frac{Q(T_{REF})}{Q(T)} \frac{\exp(-hcE/kT)}{\exp(-hcE/kT_{REF})} \frac{[1 - \exp(-hc\nu_0/kT)]}{[1 - \exp(-hc\nu_0/kT_{REF})]} \quad (7)$$

where E is the lower state energy, and Q is the temperature dependent partition function. The symbols h , c , and k are the normal fundamental physical constants. The range of temperatures experienced in this study ranged from 296 to 298 K; therefore the assumption was made that the ratio of partition functions for two closely measured temperatures is unity. Given the temperature and pressure, the pressure broadened line width is given by,

$$\gamma^p(T) = \left(\frac{T_{REF}}{T} \right)^n \left[\gamma_{air}^*(p - p_w) + \gamma_{self}^*(p) \right] \quad (8)$$

where p is the total air pressure whose value was obtained from the national weather service, n is the HITRAN temperature coefficient, and p_w is derived from independent temperature and relative humidity measurements. The * indicates that the value is for the reference temperature and pressure.

HITRAN contains many more parameters than we were able to measure, therefore the parameters were prioritized according to their importance under laboratory conditions. HITRAN parameters listed for water vapor include isotopic abundance, line position, linestrength, air-broadened half width, self broadened half width, lower state energy, line width temperature coefficient, line position pressure shift, quantum state indices, and error codes. Although our experimental platform is capable of 0.001 cm^{-1} resolution, line position and pressure shifts were not accessible due to the restriction of scanning time, changing laboratory conditions, and laser shot variability. Therefore, we imposed restrictions on scan time (i.e., resolution) and made the assumption that line positions were sufficiently accurate to use for wavelength calibration of the observed spectra. In regard to linewidths, the laboratory conditions produced lines that were predominantly widened by N_2 broadening (referred hereafter as air-broadening). Given that laboratory temperatures were near 296 K, our studies were insensitive to temperature coefficient errors. Furthermore, time constraints did not allow us to pursue temperature studies on water vapor lines, which would allow for investigations of temperature coefficient accuracy. Therefore, the parameters chosen for investigation here include linestrengths and air-broadened halfwidths.

3. RESULTS AND DISCUSSION

3.1 Experimental Layout

Figure 1 shows the optical layout of the components. The diode is a model 2010 tunable laser (Environmental Optical Sensors Inc./ Newport) and was used to control the wavelength of the alexandrite laser. The laser cavity is a piezo-tuned Littman-Metcalf external design and has a 100 kHz line-width specification. The laser head was outfitted with a DMD 765-15 model diode which has a central wavelength is 765 nm with a 30 nm spectral width. The laser beam from the diode was split 90/10 with the stronger component beam optically coupled to a single mode fiber for coupling to the alexandrite. The weaker beam was then directed to an open air white cell consisting of two confocally separated 6" f/7 gold coated mirrors and sensed with a Thorlabs Si detector with rise time 1 ns and 0.8 mm² active area. The white cell was used to detect the rotational lines of the O₂ A-band P-branch ($b^1\Sigma_g^+ (v=0) \leftarrow X^3\Sigma_g^- (v=0)$, 767 nm) for spectral location before Raman conversion of the alexandrite output. Associated with the diode laser controller is a "lock box" servo control unit which has both DC and sinusoidal modulation capability. The lock box provided DC control of the laser wavelength through the application of an offset voltage on the piezo. When modulating the wavelength, a wave function generator connected to the lock box, was used to generate a 40-50 Hz, 7 Volt peak-to-peak modulation of the diode laser piezo for course observation of the oxygen lines before fine tuning to exact peak locations.

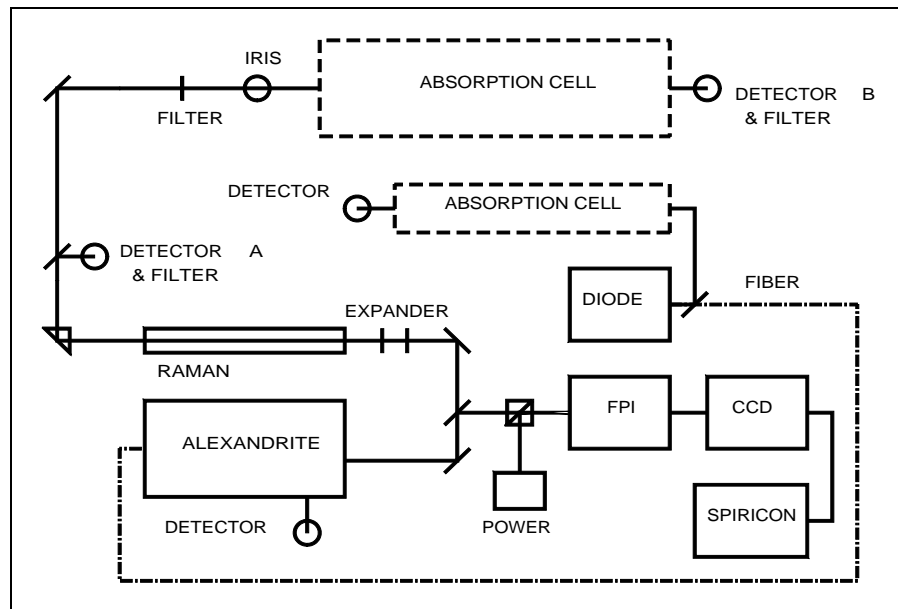


Figure 1: Optical layout of components used for spectral measurements in the 1140 nm water vapor band.

Details of the alexandrite laser cavity have been described elsewhere^{17,5,18} and only salient details will be covered here. The alexandrite laser was operated at a pulse repetition frequency of 20 Hz and provided the source for the water vapor spectroscopy measurements. The laser, when Q-switched, exhibits a 100 mJ pulse with a TEM₀₀ beam of diameter 2-3 mm. Temporally, the laser exhibited a nearly Gaussian fundamental pulse of about 180 ns in duration. Fourier transformation of the measured laser output suggested that the alexandrite laser has a line width of 10 MHz in the fundamental and 20 MHz in the 1st Stokes output. Given that the water vapor features of interest are typically not less than 1.5 GHz wide, this source has sufficiently narrow bandwidth for near-IR water vapor spectroscopy.

Wavelength tunability was accomplished through the fiber-coupling between the alexandrite cavity and the diode laser. Proper alignment and optimization of the diode laser coupling produces single mode operation of the alexandrite at the desired wavelength. When optimized, the laser wavelength can be modulated to span 4 cm⁻¹ while producing good single mode shots and minimal degradation of power.

Spectral purity of alexandrite output was monitored during data acquisition with a temperature stabilized Fabry-Perot etalon whose images were captured with a Cohu 4915 CCD camera and Spiricon laser beam profiler. The etalon has a plate separation of 15 cm and has a free spectral range of 1 GHz with a resolution of 20 MHz. In figures 2, CCD images of the spatial beam profile and Fabry-Perot interferometry are shown of the alexandrite output at 770 nm. The alexandrite

operational stability was also continuously monitored during data acquisition through photodiode and pyroelectric detection of the output pulses, which provided time resolved shot profiles and power levels.

Raman shifting of the 770 nm alexandrite laser light into the infrared (first Stokes) was achieved with a 1 meter long Raman cell (Light Age, Inc.) pressurized with hydrogen to 350 psi. Optimization of Raman conversion was desired to minimize shot-to-shot variability and pulse irregularity. This was accomplished in two ways: First, Raman conversion efficiency experiments were performed in an effort to better understand stimulated Raman scattering (SRS) processes and optimize the conversion to the 1140 nm channel. Second, the technique of external beam expansion before insertion into the Raman cell was employed to enhance conversion.

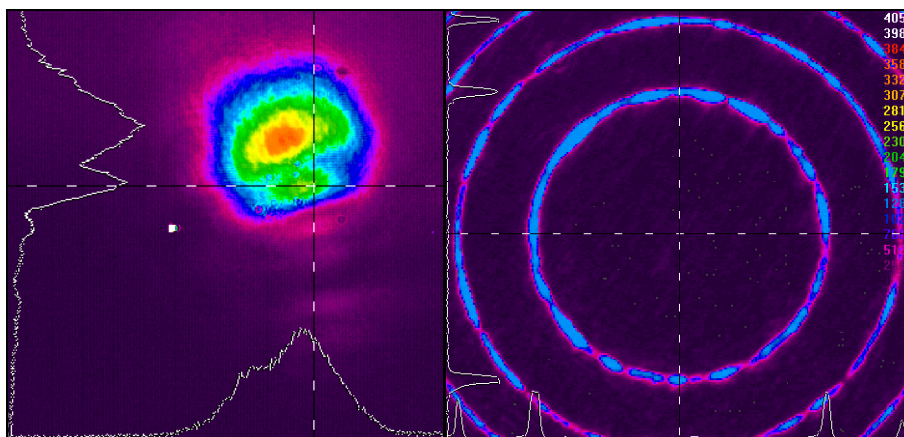


Figure 2: Spatial and spectral character of the alexandrite fundamental laser output. Both images are comprised of an average of 16 consecutive laser shots. The left picture is a spatial profile in the near field. The right picture is the image of the Fabry-Perot interferometry using a 400 mm zoom lens and the Cohu 4915 camera.

3.2 Water Vapor Measurements

The atmospheric transmittance spectrum was measured using pyroelectric detection of the filtered 1st Stokes laser light with a Laser Precision Corporation Rj-7200 Energy Radiometer. As shown in figure 1, the Raman shifted laser pulses were split into two beams in which one component was captured by detector A before insertion of the other component into the White cell. Detector B captured the second component at the output of the white cell. The instrument was later calibrated against a known transmittance and verified through independent measurement with second detection system.

A separate white cell, consisting of two 12" f/8 gold-coated mirrors with a 2.3 meter separation, was used to detect the water vapor rotational lines. The alexandrite laser beam energy was reduced at the Raman cell output with a beam splitter to avoid exceeding the recommended energy density threshold on the detectors and then spectrally filtered with a 1000 nm cutoff long pass filter. The beam was also spatially filtered with a variable iris to produce a clean single beam which was then directed into the f/8 White cell with a small 1"x2" gold coated mirror. After 53.5 meters of traversal, the beam was extracted with a small 0.5" corner cube prism. The beam was spatially filtered again at the prism with 2 mm aperture. The White cell path length was measured by time-of-flight measurement with two InGaAs detectors in the infrared.

Spectral scanning of the spectrum was done *via* DC biasing of the diode laser piezo driven cavity in 0.05 cm⁻¹ intervals. Each scan took approximately 45 minutes to acquire, covering roughly 4 cm⁻¹, and five measurements were recorded at each wavenumber interval to obtain a mean and standard deviation for each datum and associated error bar. In addition to the spectroscopic measurement, the ambient temperature and relative humidity were simultaneously measured with three different sensors whose values were subsequently used to derive temperature and water vapor concentrations. The sensors were manufactured by Hanna (HI 8064 hygrometer), Vaisala (HM141 humidity and temperature sensor), and Mannix (LAM880D temperature and humidity sensor). These instruments were later compared against an identical Vaisala model which is used for calibration at NOAA.

Fifteen lines of the 2v+δ water vapor band in the wavenumber range 8865-8915 cm⁻¹ were observed for measurement of their line strengths and air-broadened half widths. The data were taken on UT days 277-284, 2000. The measurements were made multiple times over multiple days and different path lengths to better understand the performance of the laser and variation of the atmospheric conditions in the lab. Figure 3 shows an example of the measured water absorption coefficient in the region near 8899 cm⁻¹ and the resulting best fitting model prediction (least squares sense).

Laser operational stability was not repeatable every day. Alexandrite cavity optimization, diode injection alignment, birefringent tuner adjustment, and white cell alignment had to be repeated every time a new part of the spectrum was investigated. In some scans, for example, diode mode hopping was problematic until birefringent tuner adjustment was accomplished to produce a consistent mode hop free scan. Each part of the spectrum investigated was done multiple times to get the most consistent set of results. This process was repeated for each line or set of lines. For the final set of data, only the best scans were chosen for final analysis.

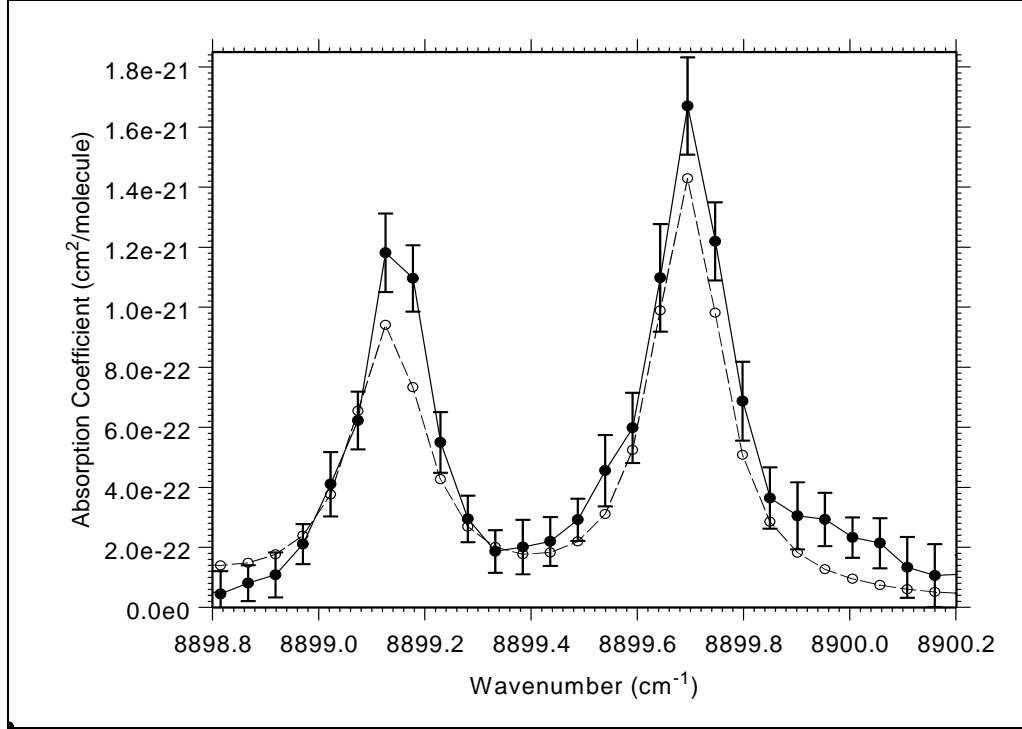


Figure 3: Example measured and modelled absorption coefficient of a pair of 1140 nm band water vapor rotational lines. The dashed line is the model and the solid line and solid circles are measured.

3.3 Comparisons with HITRAN-2000

Transmittance spectra were first converted to absorption coefficients through implementation of equation 2. Observed spectra containing multiple lines were wavenumber calibrated using the HITRAN-2000 water vapor line positions in a linear sense using two lines. In those cases where only a single line was measured, the average calibration from all multiple line measurements was used. Background correction was accomplished by fitting off-line regions in the data to the predicted values by a trial-and-error basis. Best fits between model and data were done for each individual line to avoid background error contaminating the far line fits. During this trial and error process, the sum of the square of the differences between the model and data were calculated to aid in the minimization of the least squares values.

Atmospheric transmittance data were acquired as a data set of five measurements for each wavenumber interval to obtain a mean and standard deviation. More measurements would have lengthened the time of the scan thereby increasing the susceptibility of the data to laser operational variability. Once the mean transmittance was obtained, the absorption coefficient was calculated from the measured path length and measured water vapor concentration. The line strength at the reference temperature, ($T_{REF}=296K$), was calculated using the modeled line shape parameters and then corrected for temperature:

$$S_{REF} = -\frac{A}{f_0 n_w x} \ln \left(\frac{1}{5} \sum_{i=1}^5 \tau_i \right) \frac{\exp(-hcF''/kT_{REF}) [1 - \exp(-hc\nu_0/kT_{REF})]}{\exp(-hcF''/kT) [1 - \exp(-hc\nu_0/kT)]} \quad (9)$$

Although the widths are predominantly Lorentzian, the measured widths are treated as Voigt widths. Given the measured temperature, the Doppler width was calculated and used with the measured Voigt width to calculate the total pressure-broadened width:

$$\gamma_P = \frac{\gamma_V^2 - \gamma_G^2}{\gamma_V} \quad (10)$$

Once the total pressure broadened half width was obtained, the air-broadened half width was calculated using the measured total and partial water vapor concentrations and the HITRAN tabulations for temperature coefficient and self-broadened halfwidth.

$$\gamma_{air} = \left(\frac{1}{p - p_W} \right) \left[\left(\frac{T}{T_{REF}} \right)^n (\gamma_P) - (p_W)(\gamma_{SELF}) \right] \quad (11)$$

The measured widths and peaks of the absorption features formed the central data pair from which the air-broadened halfwidths and line strengths were determined. Table 1 lists the linestrengths from HITRAN-2000, recent theoretical predictions from Nasa-Ames Research Center and the observed linestrengths, and Table 2 lists the air-broadened halfwidths from HITRAN-2000 and the observed widths. We find that the observed linestrengths compared to HITRAN-2000 are a factor of 1.28 ($\pm 13\%$) larger on average and the observed widths are larger by a factor of 1.13 ($\pm 21\%$). In figure 4, the observed linestrengths and widths are compared to HITRAN-2000 and the plot suggests that the current HITRAN linestrengths are systematically underestimated. On average, the observed widths are larger than the HITRAN entries however, the observed scatter in the data is more pronounced.

Error bars in the data were calculated from error propagation due to laser fluctuations, relative humidity and temperature measurement error, path length uncertainty, Voigt approximation error, and calibration uncertainties. Not included in the error analysis are contributions from background fluctuations that were found to be non-systematic and non-repeatable but probably only contributed to uncertainties at the 5% level. The line strength error bar was calculated from the standard deviation of the five measurements of atmospheric transmittance. This represented the shot-to-shot variability of the laser. The uncertainty in the air-broadened half-width measurement was calculated from the uncertainties in the Voigt and Gaussian components. For the Gaussian component, the error was assumed to be dominated by the uncertainty in the measured temperature. For the Voigt component, the uncertainty was calculated from the expression for the center value of the Voigt function. Since the width was measured at the half maximum value of the absorption profile, the error was assumed to be dominated by the uncertainty in the measured peak.

Table 1. Comparison of measured linestrengths to Hitran-2000 and recent work from NASA Ames Research Center.

Line (cm^{-1})	Hitran2k	Schwenke	Present work	E'' (cm^{-1})
8866.1671	1.076e-21	1.087e-21	1.46e-21 (15%)	79.496
8877.2598	5.371e-23	7.483e-23	7.46e-23 (26%)	136.762
8879.1198	5.371e-22	7.222e-22	6.33e-22 (9%)	134.902
8882.8726	3.761e-22	5.222e-22	4.77e-22 (10%)	142.279
8884.0110	1.740e-22	2.407e-22	2.09e-22 (7%)	136.164
8884.4988	2.941e-22	4.220e-22	3.81e-21 (6%)	95.176
8885.5740	1.153e-21	1.651e-21	1.47e-21 (7%)	136.762
8887.7878	5.772e-23	5.903e-23	8.62e-23 (26%)	173.365
8898.1943	9.453e-22	1.330e-21	1.14e-21 (9%)	224.838
8899.1304	2.226e-22	3.021e-22	2.89e-22 (11%)	206.301
8899.6936	3.208e-22	4.509e-22	4.25e-22 (10%)	222.052
8906.3510	8.657e-22	1.272e-21	1.04e-21 (10%)	173.365
8907.9040	8.595e-23	1.181e-22	1.15e-22 (21%)	285.219
8912.2568	2.448e-22	3.259e-22	2.64e-22 (13%)	326.625
8912.9834	7.353e-22	9.857e-22	9.12e-22 (10%)	325.348

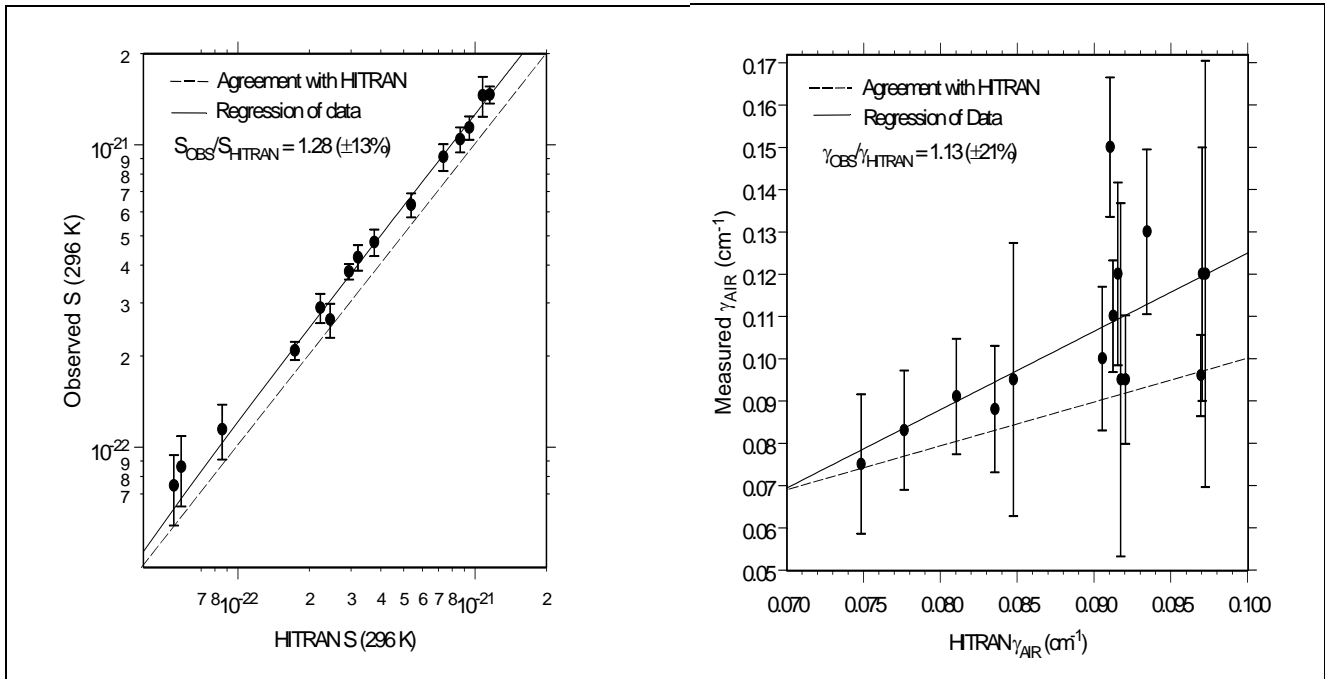


Figure 4: Measured linestrengths and air-broadened halfwidths.

Table 2. Comparison of measured air-broadened linewidths to Hitran-2000.

Line (cm^{-1})	Hitran2k	Present work	E'' (cm^{-1})
8866.1671	0.0973	0.12 (25%)	79.496
8877.2598	0.0919	0.097 (44%)	136.762
8879.1198	0.0937	0.12 (15%)	134.902
8882.8726	0.0908	0.10 (17%)	142.279
8884.0110	0.0914	0.084 (12%)	136.164
8884.4988	0.0972	0.095 (10%)	95.176
8885.5740	0.0912	0.15 (11%)	136.762
8887.7878	0.0975	0.12 (43%)	173.365
8898.1943	0.0812	0.092 (15%)	224.838
8899.1304	0.0917	0.090 (19%)	206.301
8899.6936	0.0837	0.094 (16%)	222.052
8906.3510	0.0922	0.096 (16%)	173.365
8907.9040	0.0849	0.096 (34%)	285.219
8912.2568	0.0778	0.075 (22%)	326.625
8912.9834	0.0750	0.083 (17%)	325.348

4. CONCLUSIONS

We have succeeded in the development of a narrow line, broadly tunable alexandrite based laser transmitter suitable for DIAL measurements of water vapor and temperature in the near-IR. The laser has been optimized for higher pulse energy, higher stability operation, and a nearly pure TEM₀₀ mode. The laser is seeded with a tunable diode laser whose wavelength can be modulated for high resolution scanning to 0.001 cm^{-1} . The first application of this development has been to make new measurements of selected lines 1140 nm band of H₂O. The need for spectroscopic improvements of the HITRAN database, particularly in the spectral region just beyond 1000 nm, has been established in the literature. There is now a well recognized consensus for the improvement near IR water vapor parameters, particularly important for DIAL systems under development in the US and elsewhere. Lidar profiling of atmospheric water vapor must be done with DIAL in the near-IR in order to work in daylight and over a wide range of humidities.

In this work, high resolution scans for 15 water vapor lines occurring in the range 8865-8915 cm^{-1} were used for measurement of linestrengths and air-broadened half widths. These results suggest that the lines are stronger and wider than shown in the HITRAN-2000 database. The alexandrite laser is currently configured with an output coupler which allows the water vapor spectrum to be readily accessed from 8825-8925 cm^{-1} . With the appropriate output coupler, the rubidium frequency standard would extend the operational capability to 8660 cm^{-1} . In this work, we used hydrogen for Raman conversion of the alexandrite fundamental to 1140 nm. Similar applications and studies of the H_2O band region near 940 nm can be carried out through Raman conversion in deuterium. Accurate parameters for the spectral lines of water vapor are essential for the continued development and validation water vapor lidar systems. The capability for atmospheric temperature profiling will also result from this R&D program.

ACKNOWLEDGEMENTS

The authors acknowledge the following organizations: United States Army Research Office for their generous support of this work. This work was done under ARO Contract #DAAG 55-97-1-0297. Light Age Inc. in Somerset NJ , National Oceanic & Atmospheric Administration in Boulder CO, and Nasa Ames Research Center in Sunnyvale CA.

REFERENCES

1. Rothman L.S., C.P. Rinsland, A. Goldman, S.T. Massie, D.P. Edwards, J.-M. Flaud, A. Perrin, C. Camy-Peyret, V. Dana, J.-Y. Mandin, J.Schroeder, A. McCann, R.R. Gamache, R. B. Wattson, K. Yoshino, K.V. Chance, K.W. Jucks, L. R. Brown, V. Nemtchinov, and P. Varanasi, The HITRAN molecular spectroscopic database and HAWKS (HITRAN Atmospheric Workstation): 1996 edition, *J. Quant. Spectrosc. Radiat. Transfer*, 60, 665-710, 1988.
2. Gutman W.M., W.A. Peterson, B.K. Matise, J.L. Manning, and R.E. Sulong, Atmospheric transmission spectroscopy using the sun as the source, *Appl. Optics*, Vol. 29, No. 22, August 1, 1990.
3. Belmiloud, D., R. Schermaul, K.M. Smith, N.F. Zobov, J.W. Brault, R.C.M. Learner, D.A. Newnham, and J. Tennyson, New studies of the visible and near-infrared absorption by water vapour and some problems with the HITRAN database, *Geophys. Res. Letters*, 27, No. 22, 3703 – 3706, November 15, 2000.
4. Giver L.P., C. Chackerian Jr., and P. Varanasi, Visible and near-infrared H_2^{16}O line intensity corrections for HITRAN-96, *J. Quant. Spectrosc. Radiat. Transfer*, 66, 101-105, 2000.
5. Guerra, D.V., Stimulated raman scattering in molecular hydrogen pumped by a tunable alexandrite laser, Ph.D. Thesis, The American University, Washington D.C., 1993.
6. Swensson et al., J.W., W.S. Benedict, L. Delbouille, and G. Rolan, The solar spectrum from $\lambda 7498$ to $\lambda 12016$, Institut d'Astrophysique de l'Université de Liège, Special Vol. 5, 1970.
7. Giver, L.P., B. Gentry, G. Schwemmer, and T.D. Wilkerson, Water absorption lines , 931-961 nm: selected intensities, N_2 -collision broadening coefficients, self-broadening coefficients, and pressure shifts in air, *J. Quant. Spectrosc. Radiat. Transfer*, Vol. 27, No. 4, pp. 423-436, 1982.
8. Chu, Z, T.D. Wilkerson, and U. N. Singh, Water-vapor absorption line measurements in the 940-nm band by using a Raman-shifted dye laser, *Appl. Optics*, Vol. 32, No. 6, 20 Feb. 1993.
9. Chevillard, J.-P., J.-Y. Mandin, J.-M. Flaud, and C. Camy-Peret, *Can. J. Phys.*, Vol. 67, pp. 1065-1084. 1989.
10. Lynas-Gray, A.E., S. Miller, J. Tennyson, Infrared transition probabilities for water: a comparison of ab initio and fitted dipole moment surfaces, *J. Molec. Spectrosc.*, Vol. 169, pp 458-467, 1995.
11. Partridge, H. and D.W. Schwenke, The determination of an accurate isotope dependent potential energy surface for water from extensive ab initio calculations and experimental data, *J. Chem. Phys.*, Vol. 106, No. 11, 15 March 1997.
12. Gamache, R.R., and R.W. Davies, Theoretical calculations of N_2 -broadened halfwidths of H_2O using quantum fourier transform theory, *App. Optics*, Vol. 22, No. 24, p. 4013-4019, 1983.
13. Gamache, R.R., and L.S. Rothman, Temperature dependence of N_2 -broadened halfwidths of water vapor: the pure rotation and ν_2 bands, *J. Molec. Spectrosc.*, Vol. 128, p 360-369, 1988.
14. Wulfmayer, V., J. Bösenberg, S. Lehmann, C. Senff, and St. Schmitz, Injection-seeded alexandrite ring laser: performance and application in a water-vapor differential absorption lidar, *Optics Lett.*, Vol. 20, pp. 638-640, 1995.
15. Measures, R.M., Laser remote sensing, Krieger Publishing Co., reprint edition, 1992.
16. Arnold, J.O., E.E. Whiting, and G.C. Lyle, Line by line calculations of spectra from diatomic molecules and atoms assuming a voigt line profile, *J. Quant. Spectrosc. Radiat. Transfer*, 9, 775-798, 1969.
17. Walling, J.C., O.G. Peterson, H.P. Janssen, R.C. Morris, E.W. O'Dell, Tunable alexandrite lasers, *IEEE Journal of Quantum Electronics*, Vol. 16, pp 1302-1315, 1980.
18. von Zahn, U., and J. Hoffner, Mesopause temperature profiling by potassium lidar, *Geophys. Res. Let.*, Vol. 23, No. 2, p. 141-144, Jan. 15, 1996.